
Article:
Flanagan, M., Grogan, D.M., Goggins, J. et al. (2017) Permeability of carbon fibre PEEK composites for cryogenic storage tanks of future space launchers. Composites Part A: Applied Science and Manufacturing, 101. pp. 173-184. ISSN: 1359-835X

https://doi.org/10.1016/j.compositesa.2017.06.013

Permeability of Carbon Fibre PEEK Composites for Cryogenic Storage Tanks of Future Space Launchers

M. Flanagan[a,b,c]*, D.M. Grogan[c,d], J. Goggins[a,c], S.Appel[e], K. Doyle[b,f], S.B. Leen[c,d], C.M. Ó Brádaigh[g]

a Civil Engineering, National University of Ireland, Galway, Ireland
b Engineering Department, ÉireComposites Teo., Indreabhán, Co. Galway, Ireland
c Centre for Marine and Renewable Energy Ireland (MaREI), Galway Ireland
d Mechanical Engineering, National University of Ireland Galway, Ireland
e European Space Agency / European Space Research and Technology Centre (ESTEC), Noordwijk, The Netherlands
f University of Limerick, Limerick, Ireland
g Institute for Materials and Processes, University of Edinburgh, Scotland, UK
*Corresponding Author Tel +353 89 2341401, E-mail address: M.FLANAGAN15@nuigalway.ie (M.Flanagan)

Keywords;

A. Carbon fibres; B. Permeability; D. Optical microscopy; E. Out of autoclave processing

Abstract

This work presents an experimental investigation into the permeability of carbon fibre (CF) polyetheretherketone (PEEK) for cryogenic storage tanks for space applications. The effects of cryogenic cycling, manufacturing method, PEEK matrix type, fibre type, cryogenic temperatures, pressure, and thickness on the permeability of CF-PEEK laminates are investigated. Laminates are manufactured using autoclave, press and in-situ laser assisted automated tape placement (ATP) consolidation. Optical microscopy is used to characterise the microstructure of test samples. The results show that, for undamaged autoclaved CF-PEEK samples, the permeability remains essentially constant for the ranges of pressures and thicknesses tested. Samples manufactured using the ATP process and samples which were damaged by cryogenic cycling, had a higher leak rate than autoclaved and pressed samples. For cryogenically cycled samples, the leak rate was shown to be dependent on the damage state of the microstructure.

1 Introduction

The current cost to send 1 kg of payload into geosynchronous transfer orbit using the SpaceX Falcon launcher is approximately $7500 [1]. The weight reduction achievable due to the high specific strength of carbon fibre reinforced polymers (CFRP) has led to their use in cryogenic storage applications in the space industry. Composite overwrapped pressure vessels, which consist of low permeability liners wrapped in CFRP, are currently used to store cryogens such as liquid hydrogen (LH_2) and liquid oxygen (LO_2) [2-4]. The low permeability liner, typically aluminium or titanium, limits the leakage of the cryogen, and the CFRP provides strength and stiffness to the structure. To fully exploit the potential weight saving of CFRP in cryogenic storage, the weight of the liner must be reduced or liner-less tanks must be designed. The failure of the liner-less X-33 CF-Epoxy tank, due in part to leakage in the tank walls [5], highlights the importance of understanding leakage bahaviour in the design of CFRP cryogenic storage tanks.

The term permeability has been used in the literature to refer to leak rate [6], permeability as defined by Fick's law [7-9] and permeability as defined by Darcy's law [10]. For materials that display non-Fickian behaviour, the permeability and diffusivity calculated using Fick's law are not meaningful. This illustrates that in order to present valid permeability data it must be verified that the material behaviour is close to Fickian. In this study, leak rate through the sample is reported in units of Scc/sm^2, whilst permeability and diffusivity, as defined by Fick's law, are given in units of mol/smPa and in m^2/s, respectively. Fick's law describes the transport of matter from areas of high concentration to areas of low concentration through the process of diffusion. For the testing in the current study a high concentration of helium is maintained on one side of the sample and a low concentration is maintained on the other side of the sample. This concentration gradient across the sample is the reason that molecules of helium diffuse throught the test samples. The process is charachterised by an initial time lag, as the helium diffuses through the solid sample, followed by a rise in concentration on the low pressure side until the system reaches a steady state.

Several experimental studies have investigated the leak rates of various CFRPs [6-9, 11-19]. Peddiraju, Popov, Lagoudas and Whitcomb [19] showed that leakage caused by gas flow through connected micro-cracks is typically orders of magnitude higher than leakage caused by diffusion alone. Stokes [13] stated that CFRPs in an undamaged state had an acceptable leak rate for application in cryogenic storage tanks and that the lack of success in applying CFRPs to hydrogen storage tanks is due

to micro-cracking at cryogenic temperatures. Choi and Sankar [9] showed that permeability increased by several orders of magnitude following cryogenic cycling for samples with connected micro-cracks propagating through the thickness of the samples. However, there was little change in permeability for samples where the micro-crack network did propagate through the entire thickness of the laminate to form a connected leak path. Although the damage state of the microstructure is an important factor in understanding the mechanism of leakage through composites, it is not always investigated as part of leak rate studies.

For well-consolidated, undamaged composites, the mechanism of gas leakage through the composite is diffusion. Schultheiß [8] has shown that for undamaged composites, leakage shows flux time behaviour similar to a Fickian distribution. For undamaged composites, changes in fibre volume, fibre type, resin type, temperature and the addition of nano-particles affect permeability, typically by less than an order of magnitude [7-9]. Although Fick's law is only applicable to homogeneous materials [20], undamaged composites show near-Fickian behaviour and the effect of temperature on an undamaged laminate can be expressed by an Arrhenius equation where permeability decreases with temperature [7, 21].

For damaged samples with connected leak paths, Darcy's law has been used to predict the leak rates of gas through micro-cracks [10, 22-23]. Grenoble and Gates [11] showed that mechanically cycled samples have a higher leak rate at low temperatures, furthermore it was shown that leak rate increased with both increasing micro-crack density and applied mechanical strain at both cryogenic and room temperature. Bechel, Negilski and James [6] showed that in the absence of micro-cracks there was no measurable leakage, that increasing crack densities lead to increasing leak rates, and that high fracture toughness reduced micro-cracking and leak rates. Kumazawa, Susuki and Aoki [15] showed that leak rate increased with increasing crack opening displacements caused by applied strains. For damaged samples with connected leak paths, the geometry of the leak paths, the viscosity of the test gas and the pressure difference across the sample influence the leak rate. As such, the fibre volume, fibre type, resin, layup, temperature, pressure and strain state all affect the leak rate. Goetz, Ryan and Whitaker [5] have shown that leak rates through damaged samples increase with applied strain and decreasing temperature. Temperature affects both the geometry of the leak paths, due to thermal strain, and the viscosity of the leaking gas. The pressure gradient across the sample is the reason for helium flow through samples with connected leak paths.

Thermoplastics have several advantages over thermosets; they can be manufactured using automated techniques such as Automated Tape Placement (ATP) and fusion bonding. Furthermore, they have superior toughness and storage life [24]. This has led to research into the application of thermoplastics to cryogenic storage [3-4]. Laser assisted ATP is an out of autoclave manufacturing technique, which involves automated, in-situ placement, and consolidation of CF thermoplastics with laser heating. ATP can be used to make large parts without the need to use large autoclaves which provides a potential cost benefit over thermoset production [25].

CF-PEEK, which can be manufactured using the ATP process, has been identified as a potential material for cryogenic storage tanks due to its specific strength, toughness and chemical resistance. Ahlborn [26] showed that CF-PEEK samples, manufactured with AS4 fibres, showed no micro-cracking after 120 cryogenic cycles. Funk and Sykes [27] showed that AS4-PEEK had a crack density of 0.1 cracks per millimetre after 500 cryogenic cycles and concluded that of the six CFRPs tested, AS4-PEEK was the best suited to cryogenic aerospace applications due to its resistance to micro-cracking after cryogenic cycling. Nairn [28] showed that micro-cracking of CF-PEEK followed similar trends to CF-Epoxy and the superior toughness of CF-PEEK was negated by higher residual thermal stress in the as-manufactured state.

Grogan, Leen, Semprimosching and Ó'Brádaigh [29] investigated damage formation due to cryogenic cycling in autoclave samples manufactured from three types of commercially available CF-PEEK: Suprem IM7-PEEK, Cytec IM7-PEEK, and Tencate AS4-PEEK. This work showed that (i) PEEK type affected micro-crack density with Suprem IM7-PEEK being the most susceptible to micro-cracking, (ii) for the majority of samples no further micro-cracking occurred after the first cryogenic cycle, (iii) the majority of cracks extended in the fibre direction, through the full length of the specimen and (iv) thicker samples and quasi-isotropic layups were more susceptible to cracking due to cryogenic cycling.

Nettles and Biss [30] states that in order for CFRP's to be used in cryogenic applications the permeability of these material must be characterised. The permeability and leak rate work carried out to date has focused mainly on composites with thermosetting matrices, as these have been the most common materials used in the aerospace industry. The current work compliments the work of Grogan et al. [29] by address the knowledge gap surrounding the permeability and leakage behaviour of damaged and undamaged CF-PEEK. The work investigates the leak rates of CF-PEEK from different material suppliers, composed of different fibres, and manufactured using different consolidation techniques.

Optical microscopy and 3D X-ray CT scanning are used to verify the quality of the laminates and to monitor cryogenic cycling damage to the microstructure in order to better understand the leakage behaviour of CF-PEEK. The permeability results are compared to experimental results from literature and a published allowable leak rate for cryogenic storage tanks given by Robinson [31] of 3.58 Scc/sm^2. Different cryogenic storage designs may require orders of magnitude difference in leak rate allowables, and the design allowable presented here is given for context only.

2 Methodology

2.1 Materials

Permeability tests were performed on four different CF-PEEK materials: Cytec PEEK with 60% AS4 fibres [32], Cytec PEEK with 60% IM7 fibres [32], Suprem PEEK with 60% IM7 fibres [33] and Tencate PEEK with 59% AS4 fibres [34]. Laminates were manufactured using heated press, autoclave, and laser assisted ATP consolidation. Permeability tests were also carried out on CF-M21 Epoxy [35], on un-reinforced PEEK and un-reinforced PVC in order to compare the test results to published data and validate the test methodology. The CF-Epoxy sample was cured in the autoclave in accordance with the manufacturer's specification given in [35]. The PEEK sample was manufactured by laying up several sheets of Victrex PEEK [36] film and consolidating in a heated press. Information on laminate ID, supplier, fibre type, manufacturing method and layup is given in Table 1. All CF-PEEK samples are coded in accordance with their supplier (C for Cytec, S for Suprem and T for Tencate), fibre type (4 for AS4 and 7 for IM7) and manufacturing method (AC for autoclave, P for press and ATP for automated tape placement). For example, in sample C4AC, "C" indicates that the material is supplied by Cytec, "4" indicates the fibre type is AS4, and "AC" indicates the samples were manufactured using the autoclave. The trademark of the PEEK matrix for each material system is given, but further details such as additives used during processing and manufacturing techniques is not available from suppliers. Before testing, the quality of all CF-PEEK samples was verified using ultrasonic through-transmission and optical microscopy. Test samples, of dimensions circa 200mm by 200mm, were extracted from the parent laminate using a water-cooled diamond blade. All autoclave and press laminates were processed at 380°C and a pressure of 6 bar, in accordance with the manufacturers' recommendations, in an EN/ISO 9100 [37] accredited facility. Autoclave samples experienced a cooldown rate of circa 5ºC per minute, this would lead to a crystallinity percentage of 30-35% [24]. Press laminates and the un-reinforced PEEK sample

have cooling rates of circa 1 ºC per minute which would lead to a crystallinity of 37-42% [24]. The ATP laminate was manufactured using Suprem CF-PEEK tape designed for use with the ATP process. The crystallinity percentage of the ATP specimen, measured using differential scanning calorimetry, was found to be 25% [38].

2.2 Cryogenic Cycling

Test Samples taken from laminates C4AC, C7AC, T4AC, S7AC1 and S7ATP were subjected to cryogenic cycling between -196°C and room temperature. Although LH_2 and LO_2 are typically stored in cryogenic tanks, for issues of safety and practicality, liquid nitrogen (LN_2) is commonly used for cryogenic cycling in laboratory testing. Samples were immersed in LN_2 for 2 minutes, removed, and heated to room temperature for 6 minutes using a convection fan. The cryogenic cycle was verified by embedding a thermocouple in an 8-ply laminate during a cryogenic cycle.

2.3 Test Method

All samples are tested using a Leybold L200, mass spectrometry-based, helium leak detector. Helium was used as a test gas as it has a similar molecular diameter to hydrogen and it gives similar measured permeability results to hydrogen [6-7]. The mass spectrometry test setup, shown in Fig. 1, is similar to that used previously in the investigation of permeability of composites [6-7, 14]. This test setup measures only the helium in the lower chamber. This means that the system is less susceptible to errors due to leakage from atmospheric gasses into the test chamber as noted by Bechel et al. [6]. To seal the sample in place, Viton O-rings are used for room temperature testing and indium rings are used for cryogenic temperature testing.

The samples were placed between the upper and lower test chamber and helium gas was then introduced into the upper chamber. The helium leaked through the test sample into the lower test chamber. The helium leak detector drew a vacuum in the lower chamber and measured the helium leak rate through the sample and the pressure in the lower chamber. Monitoring the pressure in the lower chamber allowed the quality of the seals to be evaluated before testing.

2.4 Procedure

Test samples were placed between the upper and lower test chamber and clamped in place using threaded fasteners. The upper chamber was evacuated using the vacuum pump shown in Fig. 1 and the lower chamber was evacuated using a pump incorporated into the leak detector. The pressure in the lower chamber was monitored to ensure that there was no leakage due to poor seals. If the pressure in the lower chamber did not drop below 0.015 millibar this indicated that the sample was not sealed correctly or the sample was leaking at a very high rate. This value was chosen as it gave a measured background signal that was one order of magnitude lower than the signal from the lowest permeability samples tested. In cases where the pressure did not drop, the sample was removed, inspected, cleaned and re-tested. If the issue continued, a low viscosity, polyurethane edge sealant was applied to the sample surface around the O-ring clamping area. Samples with a rough surface or surface damage would not seal adequately without the use of polyurethane sealant. If the pressure in the test chamber was still high following the application of polyurethane sealant, it was concluded that this was due to a high leak rate through the sample and the test was continued. The valve to the vacuum was closed and helium was introduced into the upper test chamber. The time at which the helium was introduced was recorded at the start of the test. Standard samples were exposed to helium at a pressure difference of 1 bar across the sample. Samples S7AC3, 4, and 5 were tested at a pressure difference of 1 bar and 10 bar across each sample. The test area enclosed by the O-rings for all samples was 0.0095 m^2.

Permeability testing at cryogenic temperatures was performed used the same principle as above, with indium seals being used instead of Viton. The sample was initially allowed to reach a steady state at room temperature. The test chamber was then submerged in the liquid nitrogen dewar shown in Fig. 1 and the leak rate was monitored until it reached steady state at cryogenic temperatures.

For each laminate type, testing was carried out to identify the time taken for the sample to reach steady state. The steady state time was defined as the time when leak rates reach their respective constant values without any significant fluctuations (+/-5% deviation) over a time period appropriate for the sample type. This steady state time was then set as the test time for samples of this type. Test times varied from several minutes for damaged samples to 50 hours for thick samples.

2.5 Calculation of Permeability and Diffusivity

At steady state, the permeability, *P* through a membrane, in the through thickness direction is calculated from [7, 20, 39]:

$$P = \frac{J_{ss} l}{A\,(p_u - p_l)} \qquad (1)$$

where J_{ss} is the steady state leak rate, A is the sample surface area, p_{u} is the partial pressure of permeate in the upper chamber, p_{l} is the partial pressure of permeate in the lower chamber and l is the sample thickness. In the current study, pure helium was used in the upper chamber and a high vacuum was drawn in the lower chamber so that the partial pressures are equal to the actual measured pressure. Eq. 1 is equivalent to Fick's first law [39], for the current testing, where it is assumed that the diffusivity, D, is independent of concentration, and the permeate surface concentration is proportional to the applied partial pressure.

For materials that follow Fickian behaviour, under the test conditions described above, the normalised leak rate at any time, t, is given by [39]:

$$\frac{J}{J_{ss}} = \frac{4}{\sqrt{\pi}} \sqrt{\frac{l^2}{4Dt}} \sum_{\mathrm{n}=0}^{\mathrm{n}=\infty} \exp\left\{\frac{-(2n+1)^2 l^2}{(4Dt)}\right\} \qquad (2)$$

where J is the leak rate at time t. By inputting the value of $J/J_{ss} = 0.5$ and solving for D, Eq. 2 reduces to $D = l^2/7.199t_{0.5}$, where l is the sample thickness and $t_{0.5}$ is the time taken for the leak rate to reach half its final value.

Defining the non-dimensional leak rate j as $j = J/J_{ss}$ and the non-dimensional thickness-time as $\tau = Dt/l^2$ samples with different leak rates, thickness and test times can be compared to theoretical Fickian behaviour using Eq. 2.

Although permeability as defined by Fick's law has previously been applied to composites, strictly speaking, it only applies to homogeneous materials [20]: hence, it is important to assess its validity for composite materials, on a case by case basis, by comparing the sample behaviour to theoretical Fickian behaviour.

3 Results and Discussion

This section presents results and discussion of the laminates listed in Table 1. The results are broken into three separate sections which present data on the microstructure and the leak rates of the laminates. The first section presents the results pertaining to un-cycled autoclave laminates, un-reinforced PVC and un-reinforced PEEK. These results are compared with available results from literature. The second section

presents the results pertaining to un-cycled press and ATP laminates. The third section presents results on the effect of cryogenic cycling on autoclave and ATP laminates.

3.1 Autoclave Laminates

3.1.1 Microstructure

Micrographs from laminates SC4AC, C7AC, T4AC, S7AC1 and S7AC2, were taken along a length of 200mm to examine the microstructure and to identify any processing defects. All autoclave samples were shown to have a uniform structure, consistent ply thickness and well-distributed fibres. No fibre wrinkles, de-laminations, gaps or foreign matter were observed and all samples had a measured void content less than 1%. Fig. 2 shows micrographs of laminates S7AC, T4AC, C4AC and C7AC, chosen to represent the general, well-consolidated microstructure of each laminate type. The Suprem IM7 laminate and Tencate AS4 laminates have the most homogeneous structure with fibres uniformly distributed and no large intralaminar or interlaminar resin rich areas. Both Cytec IM7 and AS4 laminates show a less homogeneous structure with fibres less uniformly distributed and intralaminar and interlaminar resin rich areas shown in dark grey. The micrographs showed that all autoclaved laminates were well consolidated, with no clusters of voids, or damage that could form a connected leak path.

3.1.2 Leak Rate

Table 2 shows a summary of the measured leak rates, permeabilities, diffusivities, and sample behaviour for autoclaved CF-PEEK, CF-Epoxy, un-reinforced PEEK and un-reinforced PVC tested at a pressure difference of 1 bar. In the case where results are based on more than one sample, the coefficient of variation (Cv) is given. One sample from laminate C4AC was tested at cryogenic temperatures in order to investigate the influence of cryogenic temperature on permeability.

The data in Table 2 shows that the leak rate of CF-PEEK for all samples is well below the allowable leak rate given in [31]. The result of testing C4AC at -196°C shows a decrease of two orders of magnitude for leak rate and permeability at cryogenic temperatures. A decrease in permeability with temperature for composite materials was reported by Humpenöder [7], who also showed that the decrease follows an Arrhenius equation. The result measured at cryogenic temperature is the lowest leak rate of all test samples measured and indicates that leakage due to diffusion through the composite at cryogenic temperatures is extremly low. At the rate measured here it would take 18 days for a volume of one

centimeter cubed at standard temperature and pressure to leak through a one meter squared area of composite (Scc/m^2). The data presented in Table 2, indicates that damage free autoclaved CF-PEEK is a suitable material choice for cryogenic storage.

Fig. 3 shows a comparison of the theoretical $j - \tau$ response, plotted using Eq. 2, with measured data from samples taken from laminates C4AC and S7ATP. The agreement between the theoretical Fickian curve and the results from laminate C4AC indicates that the assumptions used in Eq.2 are reasonable. For the purpose of this study samples shall be described as Fickian, near-Fickian and non-Fickian depending on how they compare to the theoretical $j - \tau$ curve. The behaviour of sample C4AC is described as near-Fickian as it follows the theoretical Fickian response closely. It shows an initial time lag followed by an increase in leak rate, before slowly reaching steady state bahaviour. In contrast the leak rate of sample S7ATP is described an non-Fickian as it shows an immediate increase once gas is introduced, with no initial time lag. Samples that show Fickian behaviour follow the above equations and also an Arrhenius equation where leak rate decreases with decreasing temperature [7-8].

All autoclave CF-PEEK samples tested show near-Fickian behaviour and all leak rate, permeability and diffusivity results measured at room temperature are within one order of magnitude difference, respectively. The differences in permeability and diffusivity between similar CF-PEEK materials may be due to (i) different grades of PEEK used by different suppliers, (ii) differences in supplier manufacturing techniques and (iii) different fibres and fibre sizing.

The diffusivity influences the rate at which the permeate diffuses through the samples and the time taken for the system to reach steady state. A steady state was reached by un-reinforced PEEK in circa 2 hours, by Cytec AS4 in circa 12 hours, and by Cytec IM7 in circa 20 hours.

Comparing the results of the CF-PEEK to the un-reinforced PEEK, shows that the addition of fibres to the matrix decreases the permeability in agreement with Humpenöder [7] . This decrease in permeability and increase in time taken to reach steady state for the CF- PEEK sample is likely due to the increased length of the diffusion path due to the gas having to diffuse around the fibres. This effect is known as tortuosity [40].

Fig. 4 compares the results of this study with the results from literature. The measured permeability of CF-PEEK, PVC, un-reinforced PEEK, and CF-Epoxy are in agreement with the values reported in literature. The results for CF-PEEK are also in the same range as CF-Epoxies given in literature. This shows that the permeability of the CF-PEEK is in line with thermosetting CF composites, and from the

point of view of permeability, is equally well suited to the manufacture of cryogenic storage tanks. The result presented by Choi and Sankar [9], which is unusually low, highlights the wide spread of data from literature. The spread of data in the literature could be due to the lack of a standard test method or apparatus for assessing the permeability of composites and the varying sensitivity of different test setups. The ASTM D1434 [20] test standard for measurement of the gas permeability characteristics of plastic film has been widely adopted for permeability testing of composites [9, 17, 41]. This standard states that the measurements give semi-quantitative results for the permeability and that the results are dependent on the lab test setup. The standard was updated in 2015 and an incorrect formula for calculating the gas transmission ratio has been corrected.

Fig. 5 shows the measured effects of pressure and sample thickness on permeability. Fig. 5 (a) shows the influence of pressure on leak rate and Fig. 5 (b) shows the influence of pressure on permeability for three Suprem IM7 samples, tested with a pressure difference of 1 bar and 10 bar. Laminates S7AC3, S7AC4 and S7AC5 were all manufactured in the same autoclave with the same process conditions and tooling. Fig. 5 (a) shows that the increase in pressure leads to an increase in leak rate. However, Fig. 5 (b) shows that the permeability remains constant, in line with Eq. 1. This result indicates the assumption that permeate surface concentration is proportional to the applied partial pressure is reasonable over the pressure ranges investigated. Fig. 5 (c) shows the permeability and leak rate of Suprem IM7 laminates, S7AC1, S7AC2, S7AC3, S7AC4 and S7AC5, tested at a pressure difference of 1 bar. The results show that the leak rate of the thicker laminate (S7AC2) is reduced in comparison to the other laminates. However, the permeability remains constant, in line with Eq. 1. These results have important implications for the design of composite cryo-tanks. If the permeability is measured at a certain pressure, for a certain laminate thickness, the permeability measurement can be used to predict the leak rate of proposed tank designs of different thicknesses and pressures.

3.2 ATP and Pressed Laminates

3.2.1 Microstructure

ATP and press consolidated laminates were manufactured and tested in order to assess the suitability of these manufacturing methods to cryogenic storage applications. Micrographs of laminates S7P and S7AC2 showed that the press and autoclave laminates had a similar microstructure to that shown in Fig. 2 with void contents below 1%. Micrographs of ATP laminate S7ATP show many large local defects and

several surface micro-cracks. These defects included large de-laminations, areas of foreign matter and several areas of co-incident defects of different types that occurred more frequently on the surface plies. Fig. 6 shows three surface plies of laminate S7ATP and represents the largest defect area examined during inspection; the entire defect consisted of a de-lamination 3 mm in length, a large micro-crack, foreign matter, and a void located in three surface plies of the laminate. The micrographs show that the foreign matter contains randomly orientated carbon fibres and the micro CT indicates that the scrap material has a similar density to the composite. This suggests that the foreign matter is CF-PEEK debris that has been unintentionally consolidated into the laminate during the ATP manufacturing process.

3.2.2 Leak Rate

Table 3 presents a summary of the measured leak rates, permeabilities, diffusivities, and sample behaviour for Suprem CF-PEEK laminates for each manufacturing method tested at a pressure difference of 1 bar. The data presented is based on the average of several test samples taken from each laminate and the coefficient of variance is given for each result. The leak rate, permeability, and diffusivity of the autoclave and press laminates are very close to one another, have a low coefficient of variance and show near-Fickian behaviour.

Table 3 also shows that the ATP samples do not follow Fickian behaviour, i.e. no initial time lag and behaviour similar to the non-Fickian sample in Fig. 3. The ATP laminate has a much higher leak rate than both autoclave and press laminates, it also has a coefficient of variance of leak rate of 70%, and the time taken for the samples to reach steady state was circa 2 hours. The high leak rate and coefficient of variance of ATP laminates is thought to be due to randomly located local defects which allow leakage through connected leak paths. The presence of these defects highlights possible issues with the ATP manufacturing process. Development of the ATP process parameters to eliminate these defects would lead to leak rate properties closer to that of autoclave and press laminates and Fickian behaviour.

3.3 Cryogenically Cycled Laminates

3.3.1 Microstructure

Samples taken from laminates C4AC, C7AC, T4AC, and S7AC1 were examined after 0, 1, 10, 20 and 30 cryogenic cycles. Each sample had an edge polished and inspected to investigate the effects of cryogenic cycling on the microstructure.

Samples taken from laminate C4AC showed one surface ply micro-crack before cryogenic cycling. Fig. 7 shows the micro-crack on the surface of a sample taken from laminate C4AC before and after cryogenic cycling, which shows no discernible change in this micro-crack between 0 and 30 cycles. This indicates that for laminate C4AC, the observed individual crack did not propagate following cryogenic cycling.

Samples taken from laminate C7AC showed no micro-cracks before cryogenic cycling and 3 surface ply micro-cracks following cryogenic cycling. The micro-cracks were similar to that shown in Fig. 7.

Samples taken from laminate T4AC showed no micro-cracks before cryogenic cycling and no change in microstructure following cryogenic cycling.

Samples taken from laminate S7AC1 showed no micro-cracking before cycling but all samples had micro-cracks following 1 cycle. Fig. 8 (a) shows a typical micro-crack, found in sample S7AC1, which propagates through the four central plies of the laminate. For sample S7AC1, nearly all cracks were at least 1 ply thick. Table 4 gives micro-crack densities for laminate S7AC1, following 1 cryogenic cycle (cracks less than 1 ply thick were discounted). It can be seen that there was a large difference in the crack densities from sample to sample and that not all samples had detectable cracks in all plies. Even in individual samples with high levels of damage, cracks did not show a uniform distribution, but tended to occur in unevenly spaced clusters with no discernible edge effects. Samples showed no change in micro-crack density after the first cryogenic cycle. The lower Mode I and Mode II fracture toughness of Suprem IM7-PEEK (1515 and 1355 J/m^2 [42]) when compared to Cytec IM7-PEEK (2300 and 1900 J/m^2 [32]) has been suggested as an explanation for Suprem CF-PEEK laminates exhibiting micro-cracking after just one cryogenic cycle [29].

ATP samples examined following 1 cryogenic cycle showed micro-cracks in all samples. Micro-cracks were shorter and less defined than in autoclave samples and were sometimes indistinguishable from other defects such as areas of porosity and de-laminations as shown in Fig. 8(b). Micro-cracks did not propagate from ply to ply as with the blocked plies shown in Fig. 8(a). This is thought to be due to the layup of the laminates.

Sections from laminates C4AC, C7AC, T4AC, S7AC, and S7ATP were scanned using micro computed tomography after cryogenic cycling and post processed using the image processing package Fiji [43-44] in order to give a qualitative assessment of laminate features. The section taken from laminate

C4AC, C7AC and T4AC showed uniform structure throughout the section, indicating that the laminates were well consolidated with few voids or defects. The microstructure of laminate S7ATP was distinctive from all other laminates scanned as it showed voids, running parallel to the fibres. This indicating that there were defects, possibly caused by inaccurate tow placement during the ATP process, which ran along the direction of the fibre tows.

Fig. 9 shows ply-by-ply plan view sections of sample S7AC in which the fibre direction can be identified in most of the images. Fig. 9 also shows two micro-cracks, labelled "A" and "B", in the four central plies, which travel along the full length of the scanned section in the fibre direction. The presence of micro-cracks identified by "A", and "B" in Fig. 9 was confirmed by optical microscopy.

3.3.2 Leak Rate

Table 5 shows a summary of the measured leak rate, permeability and diffusivity of laminates S7ATP, S7AC1, T4AC, C7AC and C4AC after cryogenic cycling. Comparing these results with results for un-cycled laminates, given in Table 2, shows that cryogenic cycling has very little effect on the leak rate and permeability of Cytec AS4, Cytec IM7 and Tencate AS4. However, it increases the leak rate of Suprem autoclaved and ATP laminates by several orders of magnitude after just one cryogenic cycle. The leak rate time response for laminate S7AC1 also changes from near-Fickian to non-Fickian and the time taken to reach steady state is reduced from hours to several minutes. This indicates that leakage has changed from a diffusion-based process, driven by concentration gradient, to fluid flow through connected leak paths, driven by pressure gradient.

Fig. 10 shows the leak rate following cryogenic cycling for three samples taken from laminate S7AC1, plotted against the average crack density for each sample, taken from Table 4. Fig. 10 shows a correlation between micro-crack density and leak rate after both 1 and 30 cycles. This correlation indicates that gas flows through a connected micro-crack network, which explains the increase in leak rate, and why the leakage behaviour of damaged samples changes from near-Fickian to non-Fickian. The increase in leak rate from 1 cycle to 30 cycles also suggests that, although the crack density remains constant, further damage is caused after the first cycle. This damage may be due to propagation of internal delamination's or changing crack geometry, but further work is needed to confirm this. This result clearly highlights that micro-crack density alone cannot be used to predict leakage. The leak rate at 1 bar pressure difference is below the allowable leak rate given by Robinson [31]. However, the effect of increasing the

pressure or decreasing the temperature cannot be predicted using Ficks law as the sample deos not show Fickian behaviour.

4 Conclusions and Future Work

The permeability of four different CF-PEEK composites, manufactured using autoclave, press and automated tape placement, was measured at room temperature and after cryogenic cycling. Optical microscopy and CT scans were carried out to investigate the effect of micro-structural defects and/or cryogenic damage on permeability.

The results show that:

- The permeability of CF-PEEK is low enough to make it a suitable material choice for cryogenic storage. However, for damaged CF-PEEK, or CF-PEEK with manufacturing defects, Fickain diffusion is not the dominant leakage machanism and the leak rate must be evaluated under working conditions and compared to design allowables if these materials are to be used in cryogenic storage applications.
- All autoclaved CF-PEEK laminates showed near-Fickian behaviour before cryogenic cycling. This result allows the leak rate of proposed tank designs of different wall thickness and at different pressures to be calculated using Fick's law, provided the material is not likely to be subject damage that would lead to the creation of leakage paths during its lifetime.
- The permeability of un-cycled CF-PEEK at -196°C is several orders of magnitude less than that measured at room temperature. This shows that, for Fickian materials, using values for permeability measured at room temperature is extremely conservative.
- ATP samples showed a high leak rate (relative to un-cycled autoclave samples), high sample variance, and non-Fickian behaviour in the as-manufactured state. This was attributed to manufacturing defects in the laminates.
- Supreme IM7 micro-cracks following just one cryogenic cycle. This is in agreement with previous work carried out by Grogan et al [29]. Following cryogenic cycling Suprem IM7 showed non-Fickian behaviour and a high leak rate (relative to un-cycled samples), which was shown to correlate with micro-crack density.

- For all samples, cryogenic cycling had little effect on the leak rate of CF-PEEK unless cycling caused micro-cracking of the composite matrix.

Future work should focus on:

- Modelling micro-cracking and leak rate in composite materials. This could be carried out by importing CT scans into finite element software, as demonstrated by Harrison et al. [45] and modelling micro-crack growth using X-FEM. The effect of cryogenic temperatures and the predicted operational loads could be simulated. The results of these simulations could be used to model leakage of LH_2 and LO_2 using computational fluid dynamics. The model could be validated at room temperature using the current test setup.
- Investigating the feasibility of polymer liners. The current work has shown that permeability is reduced at cryogenic temperatures. A thin polymer liner, which remains intact following cryogenic cycling, would reduce the leak rate of damaged composites by orders of magnitude with a negligible weight penalty.
- Designing, manufacturing and testing of ATP, CF-PEEK structures to demonstrate their suitability to load bearing applications such as structural cryogenic storage tanks.

5 Acknowledgements

This research is funded by the Irish Research Council (IRC) employment based postgraduate scheme, the European Space Agency, and Science Foundation Ireland (SFI) through the MaREI centre (grant no. 12RC2302).

References

[1] SPACEX. Capabilities and Services, http://www.spacex.com/about/capabilities; 2015,[Accessed 30/12/2015].

[2] Schutz JB. Properties of composite materials for cryogenic applications. Cryogenics. 1998;38(1):3-12.

[3] Murray BR, Leen SB, Ó Brádaigh CM. Void distributions and permeability prediction for rotationally moulded polymers. Proceedings of the Institution of Mechanical Engineers, Part L: Journal of Materials Design and Applications. 2014;229(5):403-18.

[4] Murray BR, Leen SB, Semprimoschnig CO, Ó Brádaigh CM. Helium permeability of polymer materials as liners for composite overwrapped pressure vessels. Journal of Applied Polymer Science. 2016;133(29).

[5] Goetz R, Ryan R, Whitaker AF. Final report of the X-33 liquid hydrogen tank test investigation team. NASA technical report. Huntsville, Marshall Space Flight Center, NASA, 2000.

[6] Bechel VT, Negilski M, James J. Limiting the permeability of composites for cryogenic applications. Composites Science and Technology. 2006;66(13):2284-95.

[7] Humpenöder J. Gas permeation of fibre reinforced plastics. Cryogenics. 1998;38(1):143-7.

[8] Schultheiß D. Permeation barrier for lightweight liquid hydrogen tanks. [PhD], University Augsburg, 2007.

[9] Choi S, Sankar BV. Gas permeability of various graphite/epoxy composite laminates for cryogenic storage systems. Composites Part B: Engineering. 2008;39(5):782-91.

[10] Roy S, Benjamin M. Modelling of permeation and damage in graphite/epoxy laminates for cryogenic fuel storage. Composites Science and Technology. 2004;64(13–14):2051-65.

[11] Grenoble RW, Gates TS, Hydrogen permeability of polymer matrix composites at cryogenic temperatures, Proceeding of 46th AIAA/ASME/ASCE/AHS/ASC Structures, Structural Dynamics and Materials Conference. Austin, Texas, 2005.

[12] Rivers HK, Sikora JG, Sankaran SN, Detection of micro-leaks through complex geometries under mechanical load and at cryogenic temperature. Proceedings of the 42nd AIAA/ASME/ASCE/AHS/ASC Structures, Structural Dynamics and Materials Conference. Seattle, WA, 2001.

[13] Stokes EH, Hydrogen permeability of polymer based composite tank material under tetra-axial strain. 5th Conference on Aerospace Materials, Processes, and Environmental Technology. Huntsville, Alabama, 2002.

[14] Raffaelli L. Thermomechanics of fibre reinforced epoxies for cryogenic pressurized containment [PhD]. Universität München, 2006.

[15] Kumazawa H, Susuki I, Aoki T. Gas leakage evaluation of CFRP cross-ply laminates under biaxial loadings. Journal of Composite Materials. 2006;40(10):853-71.

[16] Morimoto T, Shimoda T, Morino Y, Hayashi Y, Yokozeki T, Ishikawa T. Pressurizing test of CFRP model tank in cryogenic temperature. 10th AIAA/NAL-NASDA-ISAS International Space Planes and Hypersonic Systems and Technologies Conference. Kyoto, 2001.

[17] Grimsley BW, Cano RJ, Johnston NJ, Loos AC, McMahon M. Hybrid composites for LH2 fuel tank structure. NASA technical report, 20040086019,2001.

[18] Carrión J. Composite materials for future launcher applications: Testing to meet requirements from cryogenic to hot Temperatures. European Conference on Spacecraft Structures, Materials and Mechanical Testing. Nordwijk, Netherlands, 2001.

[19] Peddiraju P, Popov P, Lagoudas DC, Whitcomb JD. Characterization of effective permeability of cryogenic composite laminates. Proceedings of IMECE'03, 2003 ASME International Mechanical Engineering Congress & Exposition. Washington, DC, 2003.

[20] ASTM. D1434-82 Determining Gas Permeability Characteristics of Plastic Film and Sheeting (reapproved 2015). Annual Book of ASTM Standards. 1982.

[21] Disdier S, Rey JM, Pailler P, Bunsell AR. Helium permeation in composite materials for cryogenic application. Cryogenics. 1998;38(1):135-42.

[22] Nair A, Roy S. Modeling of permeation and damage in graphite/epoxy laminates for cryogenic tanks in the presence of delaminations and stitch cracks. Composites Science and Technology. 2007;67(11):2592-605.

[23] Sankar B., Xu J, Van Pelt J. Lightweight composite tanks for liquid hydrogen storage. Nasa/CR – 2008-215440/Part 3, Department of Mechanical & Aerospace Engineering, University of Florida, Gainesville; 2008.

[24] Cogswell FN. Thermoplastic Aromatic Polymer Composites: A Study of the Structure, Processing and Properties of Carbon Fibre Reinforced Polyetheretherketone and Related Materials. Butterworth Heinemann Ltd, Oxford. Great Britian 1992.

[25] Pitchumani R, Ranganathan S, Don RC, Gillespie JW, Lamontia MA. Analysis of transport phenomena governing interfacial bonding and void dynamics during thermoplastic tow-placement. International Journal of Heat and Mass Transfer. 1996;39(9):1883-97.

[26] Ahlborn K. Durability of carbon fibre reinforced plastics with thermoplastic matrices under cyclic mechanical and cyclic thermal loads at cryogenic temperatures. Cryogenics. 1991;31(4):257-60.

[27] Funk JG, Sykes Jr GF. The Effects of Simulated Space Environmental Parameters on Six Commercially Available Composite Materials. NASA Technical Paper 2906, NASA, 1989.

[28] Nairn JA. Matrix micro-cracking in composites. In: Talreja R., Manson J.A., editors. Comprehensive Composite Materials Vol 1: Polymer matrix composites, Elsevier, Amsterdam, 2000. p. 403-32.

[29] Grogan DM, Leen SB, Semprimoschnig COA, Ó Brádaigh CM. Damage characterisation of cryogenically cycled carbon fibre/PEEK laminates. Composites Part A: Applied Science and Manufacturing. 2014;66:237-50.

[30] Nettles AT, Biss EJ. Low temperature mechanical testing of carbon-fiber/epoxy-resin composite materials. NASA Technical Paper 3663, NASA, Huntsville, Alabama, 1996.

[31] Robinson MJ. Determination of allowable hydrogen permeation rates for launch vehicle propellant tanks. Journal of Spacecraft and Rockets. 2008;45(1):82-9.

[32] Cytec. Technical DataSheet APC 2 PEEK Thermoplastic Polymer. https://www.cytec.com/sites/default/files/datasheets/APC-2_PEEK_031912-01.pdf; 2016,[Accessed 4/1/2016].

[33] Suprem. Suprem IM7 PEEK Material Datasheet. Supplied by Suprem: https://www.suprem.ch/.

[34] Tencate. Product Datasheet TenCate Cetex® TC1200 PEEK Resin System. http://www.tencate.com/emea/Images/CETEX-TC1200_DS_071515_Web_tcm28-3782.pdf, [Accesses 25/10/2016].

[35] Hexcel. Hexply M21 Material Datasheet. http://www.aerospares.hu/files/hexcel/hexply_m21.pdf, [Accessed 25/10/2016].

[36] Victrex. Victrex PEEK Datasheet. Supplied by Victrex: https://www.victrex.com .

[37] BSI. AS/EN 9100 Quality Managment Series Aviation Space and Defence, http://www.bsigroup.com/en-GB/as-9100-9110-9120-aerospace/; 2015, [Accessed 24/10/2016].

[38] Flanagan M. Crystallinity DSC Testing - Permeability Samples. Doc no EC0942-285-1. EireComposites, Indreabhán, Co. Galway, Ireland, 2016.

[39] Crank J. The Mathematics of Diffusion, Second Edition. Oxford university press, Bristol, England 1975.

[40] Van Rooyen, LJ, Karger-Kocsis, J, Vorster, OC, Kock, LD. Helium gas permeability reduction of epoxy composite coatings by incorporation of glass flakes. Journal of membrane science 430. 2013; 203-210.

[41] Herring HM. Characterization of thin film polymers through dynamic mechanical analysis and permeation. NASA technical paper, NASNCR-2003-2 12422. NASA, 2003.

[42] Kilroy J. New carbon fibre/PEEK composites for space applications final test report. Doc no 02/025. CTL Tástáil Teo, Indreabhán, Co. Galway, Ireland, 2006.

[43] Schindelin J, Arganda-Carreras I, Frise E, Kaynig V, Longair M, Pietzsch T., et al. Fiji: an open-source platform for biological-image analysis. Nature methods. 2012;9(7):676-82.

[44] Shneider CA, Rasband WS, Eliceiri KW. NIH Image to ImageJ: 25 years of image analysis. Nature methods. 2012;9(7):671-5.

[45] Harrison NM, McDonnell PF, O'Mahoney DC, Kennedy OD, O'Brien FJ, McHugh PE. Heterogeneous linear elastic trabecular bone modelling using micro-CT attenuation data and experimentally measured heterogeneous tissue properties. Journal of Biomechanics. 2008;41(11):2589-96.

[46] Evans D, Robertson S, Walmsley S, Wilson J. Measurement of the permeability of carbon fibre/PEEK composites. Cryogenic Materials. 1988;2:755-63.

[47] Brandrup J, Immergut EH, Grulke EA, Abe A, Bloch DR. Polymer handbook. Wiley, New York, 1999.

Tables and Figures

Table 2 Leak rates, permeability, diffusivity and sample behaviour for CF-PEEK autoclaved laminates of similar thickness, CF-Epoxy Laminate of similar layup but different thickness an, un-reinforced PEEK and PVC all tested at 1 bar.

Table 3 Leak rates, permeability, diffusivity and sample behaviour for autoclave (AC) Press (P) and automated tape placed (ATP) laminates.

Table 4 Micro-crack densities in cracks per mm for three test samples taken from laminate S7AC1 following one cryogenic cycle. No difference in micro-crack densities was found following 30 cycles.

Table 5 Leak rates, permeability, diffusivity and sample behaviour for autoclaves and ATP laminates following cryogenic cycling.

Table 6 Laminate ID, material details, manufacturing method, layup and laminate thickness of all materials tested as part of the current work.

Laminate ID	Supplier/PEEK Type	Fibre	Manufacture Method	Layup	Thickness mm
C4AC	Cytec APC 2	AS4	Autoclave	$[45°,135°,0°_4,135°,45°]$	1.1±0.1
C7AC	Cytec APC 2	IM7	Autoclave	$[45°,135°,0°_4,135°,45°]$	1.1±0.1
T4AC	Tencate Cetex TC 1200	AS4	Autoclave	$[45°,135°,0°_4,135°,45°]$	1.1±0.1
S7AC1	Suprem Victrex 150 UF 10	IM7	Autoclave	$[45°,135°,0°_4,135°,45°]$	1.2±0.1
S7ATP	Suprem Victrex 150 UF 10	IM7	ATP	$[135°,45°,90°,0°,90°,0°,90°,0°,90°]_s$	2.7±0.1
S7P	Suprem Victrex 150 UF 10	IM7	Press	$[135°,45°,90°,0°,90°,0°,90°,0°,90°]_s$	2.5±0.1
S7AC2	Suprem Victrex 150 UF 10	IM7	Autoclave	$[135°,45°,90°,0°,90°,0°,90°,0°,90°]_s$	2.3±0.1
S7AC 3,4,5	Suprem Victrex 150 UF 10	IM7	Autoclave	$[0°,90°,45°,135°]_s$	1.1±0.1
CF-Epoxy	Hexcel M21	IMA	Autoclave	$[45°,135°,0°_4,135°,45°]$	2.55±0.2
PEEK	Victrex	NA	Press	NA	1.4±0.05
PVC	NA	NA	NA	NA	1±0.1

Table 7 Leak rates, permeability, diffusivity and sample behaviour for CF-PEEK autoclaved laminates of similar thickness, CF-Epoxy Laminate of similar layup but different thickness an, un-reinforced PEEK and PVC all tested at 1 bar.

Laminate	*No of*	*Leak rate*		*Permeability*		*Diffusivity*		*Behaviour*
	samples	$\bar{x}$*(Scc/sm2)*	*Cv(%)*	$\bar{x}$*(mol/smPa)*	*Cv(%)*	$\bar{x}$*(m2/s)*	*Cv(%)*	
C4AC	4	8.5×10^{-5}	4	4.3×10^{-17}	5	1.9×10^{-11}	4	Near-Fickian
C4AC[a]	1	6.5×10^{-7}	-	3.2×10^{-19}	-	-	-	-
C7AC	4	5.2×10^{-5}	15	2.6×10^{-17}	15	9.5×10^{-12}	8	Near-Fickian
T4AC	3	1.1×10^{-4}	1	5.5×10^{-17}	1	1.7×10^{-11}	8	Near-Fickian
S7AC1	4	7.0×10^{-5}	8	4.0×10^{-17}	8	1.8×10^{-11}	16	Near-Fickian
CF-Epoxy	1	1.3×10^{-5}	-	1.5×10^{-17}	-	1.2×10^{-11}	-	Near-Fickian
PEEK	1	9.0×10^{-4}	-	5.6×10^{-16}	-	1.6×10^{-10}	-	Fickian
PVC	1	1.6×10^{-3}	-	6.8×10^{-16}	-	2.5×10^{-10}	-	Fickian

[a]Tested at -196°C

Table 8 Leak rates, permeability, diffusivity and sample behaviour for autoclave (AC) Press (P) and automated tape placed (ATP) laminates.

Laminate	*No of*	*Leak rate*		*Permeability*		*Diffusivity*		*Behaviour*
	samples	$\bar{x}$ *(Scc/sm²)*	*Cv(%)*	$\bar{x}$ *(mol/smPa)*	*Cv(%)*	$\bar{x}$ *(m²/s)*	*Cv(%)*	
S7AC2	3	3.3×10^{-5}	3	3.8×10^{-17}	3	2.2×10^{-11}	1	Near-Fickian
S7P	4	4.3×10^{-5}	9	2.4×10^{-17}	9	1.7×10^{-11}	4	Near-Fickian
S7ATP	4	8.7×10^{-4}	70	NA	NA	NA	NA	Non-Fickian

Table 9 Micro-crack densities in cracks per mm for three test samples taken from laminate S7AC1 following one cryogenic cycle. No difference in micro-crack densities was found following 30 cycles.

	Average cracks/mm	*Ply 1*	*Ply 2*	*Ply 3*	*Ply 4*	*Ply 5*	*Ply 6*	*Ply 7*	*Ply 8*
Sample S7AC1 S1	0.03	0.08	0.00	0.02	0.02	0.02	0.02	0.00	0.06
Sample S7AC1 S2	0.26	0.23	0.41	0.23	0.22	0.22	0.25	0.25	0.30
Sample S7AC1 S3	0.15	0.27	0.21	0.12	0.14	0.14	0.12	0.12	0.06

Table 10 Leak rates, permeability, diffusivity and sample behaviour for autoclaves and ATP laminates following cryogenic cycling.

Laminate	*No of*	*Leak rate*		*Permeability*		*Diffusivity*		*Behaviour*
	cycles	$\bar{x}$ *(Scc/sm²)*	*Cv(%)*	$\bar{x}$ *(mol/smPa)*	*Cv(%)*	$\bar{x}$ *(m²/s)*	*Cv(%)*	
C4AC	1	8.8×10^{-5}	4	4.5×10^{-17}	4	1.9×10^{-11}	3	Near-Fickian
	10	9.2×10^{-5}	3	4.6×10^{-17}	4	1.9×10^{-11}	7	Near-Fickian
	30	1.0×10^{-4}	11	5.0×10^{-17}	11	2.1×10^{-11}	4	Near-Fickian
C7AC	1	4.6×10^{-5}	5	2.3×10^{-17}	6	8.9×10^{-12}	9	Near-Fickian
	10	4.9×10^{-5}	6	2.4×10^{-17}	7	8.6×10^{-12}	6	Near-Fickian
	30	6.6×10^{-5}	19	3.2×10^{-17}	19	9.8×10^{-12}	4	Near-Fickian
T4AC	1	9.9×10^{-5}	7	4.9×10^{-17}	7	1.6×10^{-11}	6	Near-Fickian
	10	1.0×10^{-4}	6	5.2×10^{-17}	6	1.7×10^{-11}	7	Near-Fickian
	30	1.0×10^{-4}	6	4.9×10^{-17}	6	1.6×10^{-11}	11	Near-Fickian
S7AC1	1	2.6×10^{-1}	98	NA	NA	NA	NA	Non-Fickian
	10	7.6×10^{-1}	69	NA	NA	NA	NA	Non-Fickian
	30	8.6×10^{-1}	70	NA	NA	NA	NA	Non-Fickian
S7ATP	1	1.9×10^{-1}	52	NA	NA	NA	NA	Non-Fickian

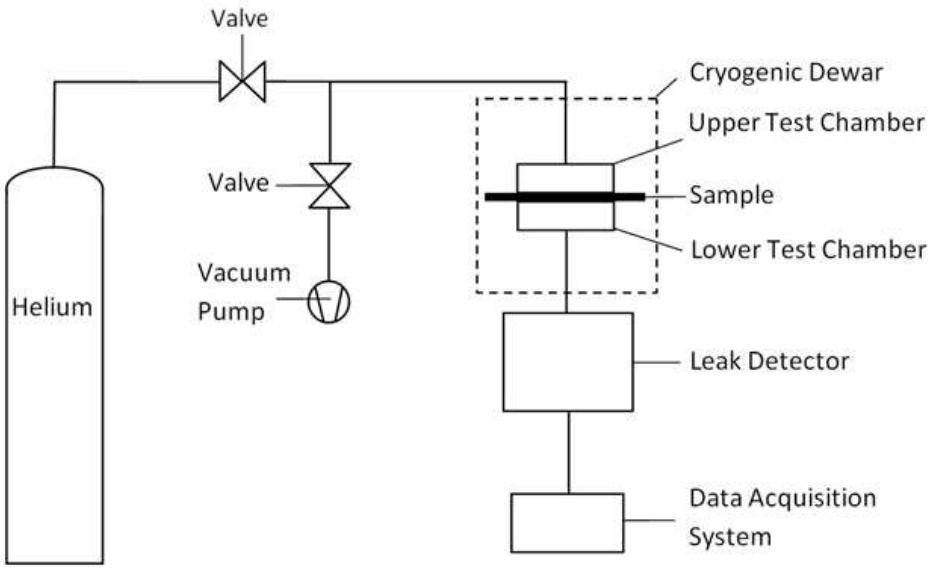

Fig. 11 Schematic of test setup used for leakage testing of laminates showing the helium gas supply, test chamber, cryogenic dewar, leak detector and the data acquisition system.

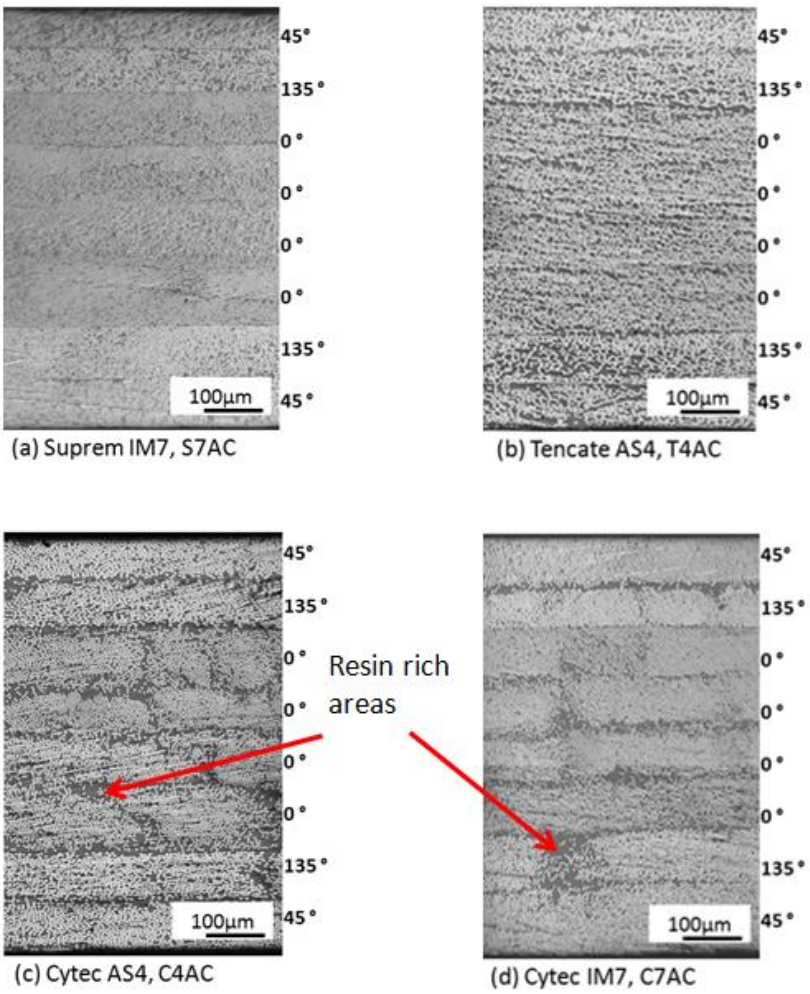

Fig. 12 Micrographs of laminates S7AC, T4AC, C4AC, and C7AC showing the layup and microstructure of each CF-PEEK material.

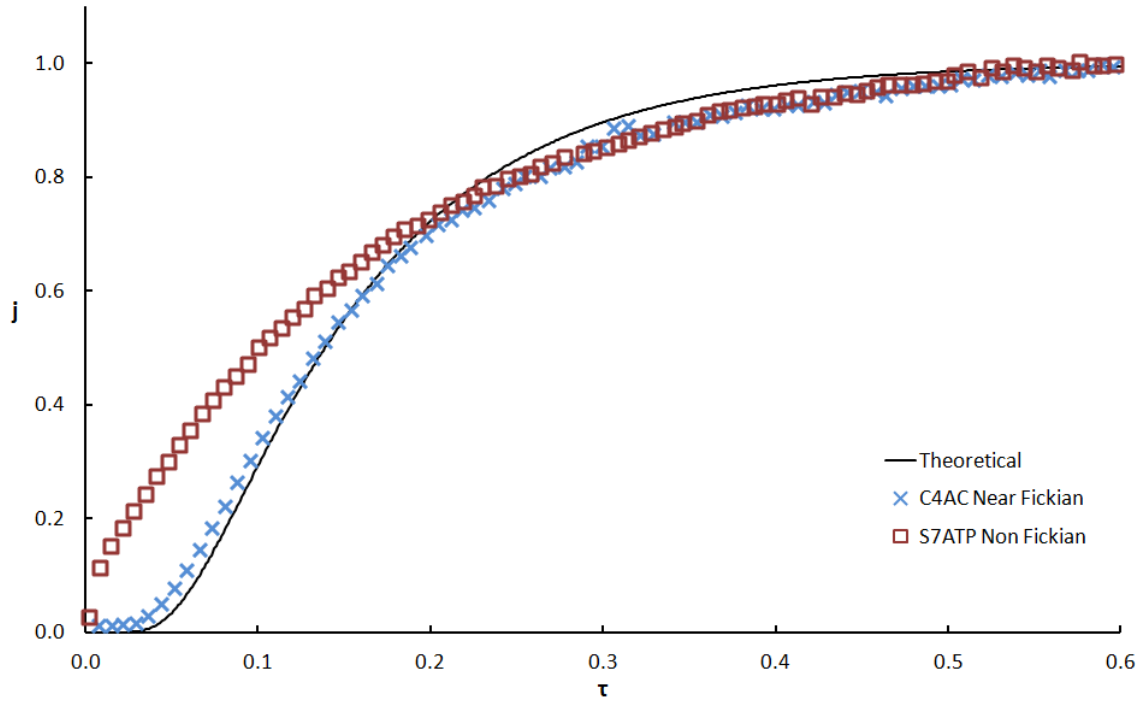

Fig. 13 The non-dimensional leak rate j *plotted against non-dimensional time and thickness* τ *for (i) theoretical Fickian behaviour, (ii) a near-Fickian Cytec AS4 autoclaved sample and (iii) a non-Fickian Suprem IM7ATP sample.*

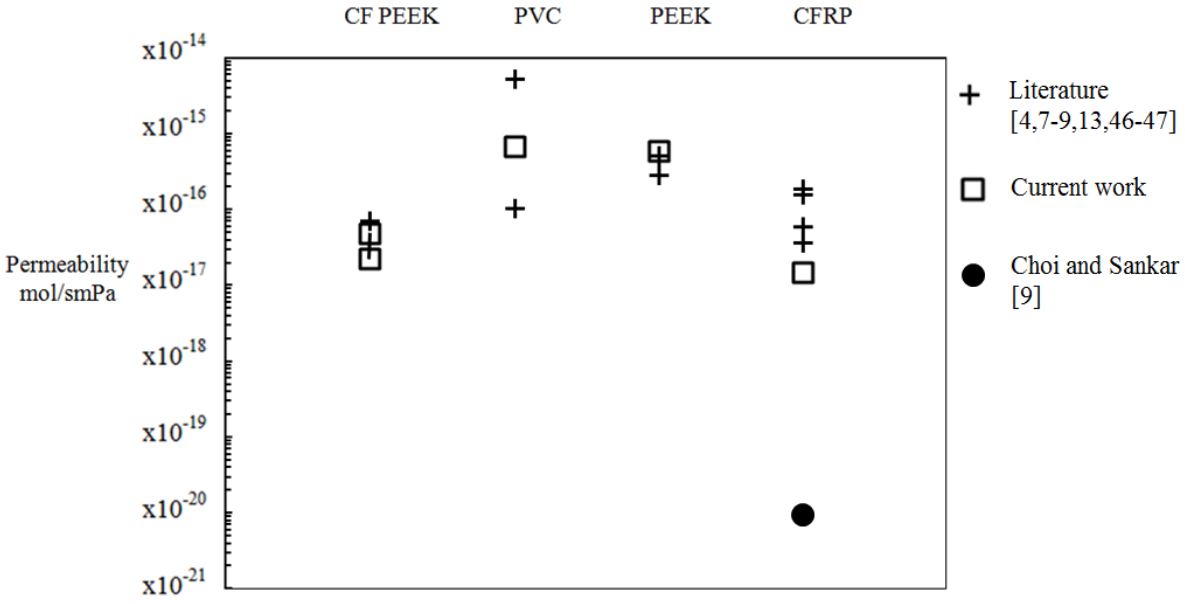

Fig. 14 Comparison of the permeability results from the current work with results reported in literature for CF-PEEK, PVC, un-reinforced PEEK, and CF-Epoxy. The minimum and maximum values for CF-PEEK from the current work are presented [4, 7-9, 13, 46-47].

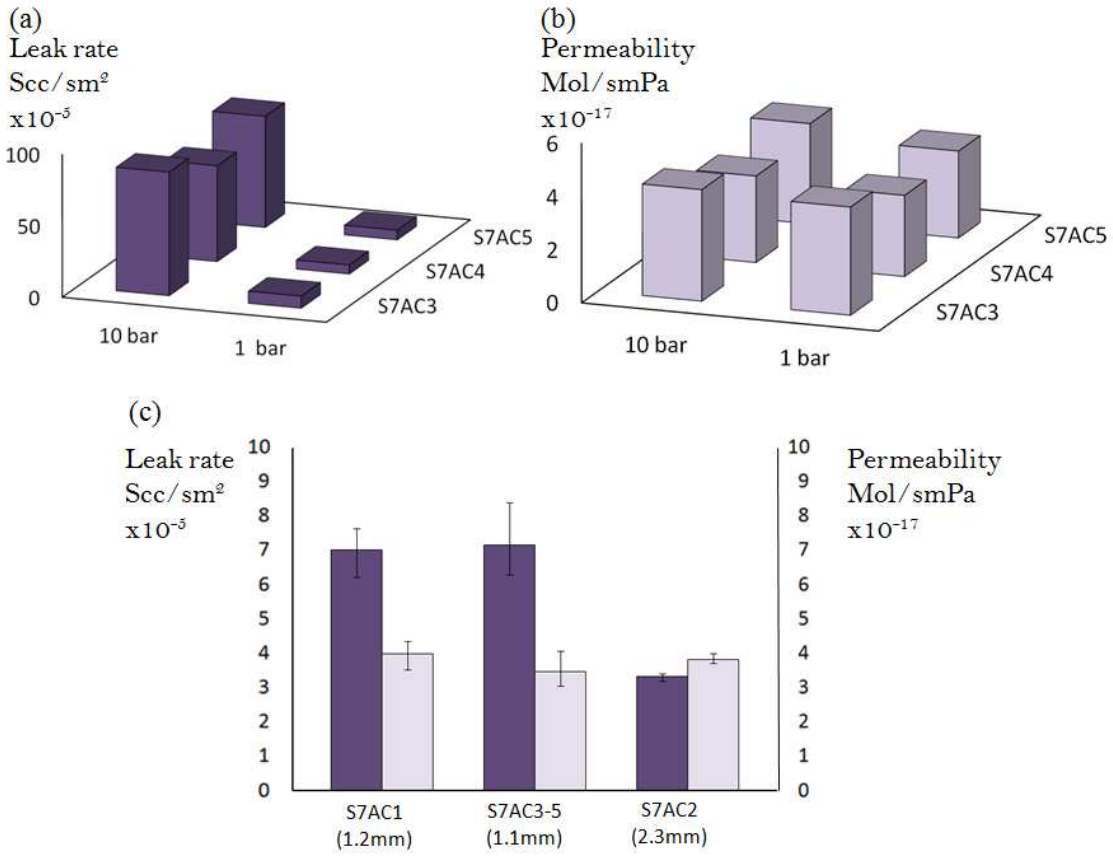

Fig. 15 (a) Leak rate of three samples tested at pressure differences of 1 bar and 10 bar, which shows that the leak rate increases with increasing pressure. (b) Permeability of three samples tested at a pressure difference of 1 bar and 10 bar, which shows that the permeability remains constant at different pressures in line with Fick's law. (c) Leak rate and permeability of samples of different thickness, which shows that leak rate decreases with increasing sample thickness, but the permeability remains constant, in line with Fick's law.

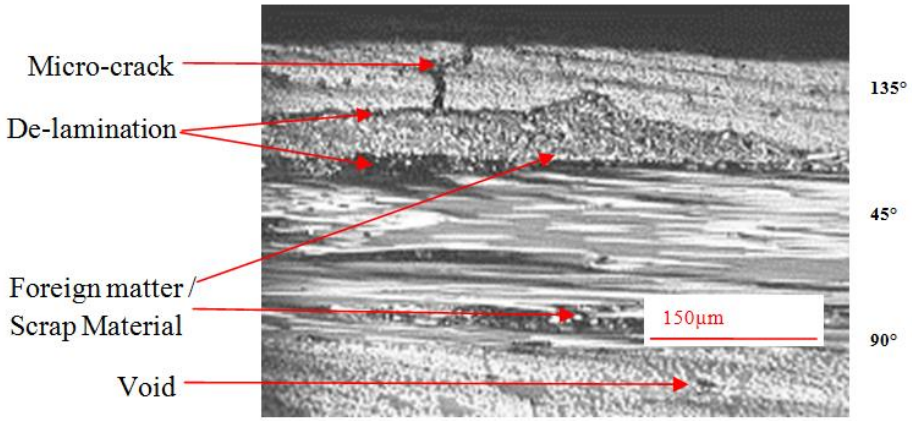

Fig. 16 Micrograph of laminate S7ATP showing a micro-crack, a large de-lamination, a void and scrap material.

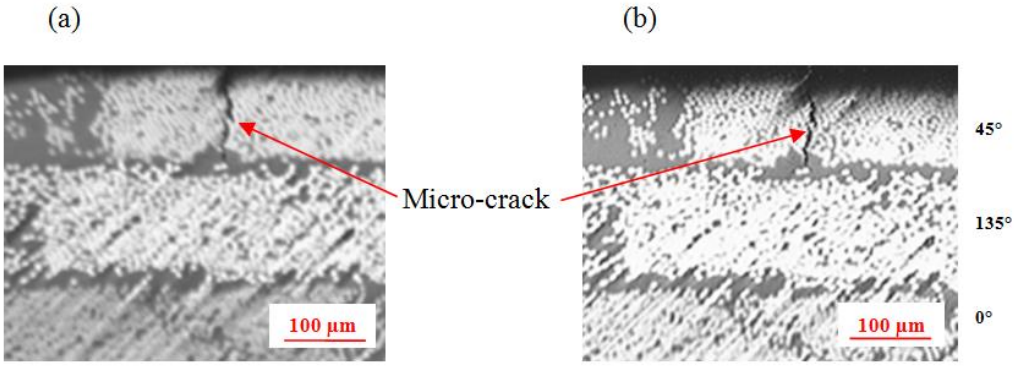

Fig. 17 (a) Micrograph of laminate C4AC showing micro-crack on surface ply before cryogenic cycling. (b) Micrograph showing the same micro-crack after 30 cryogenic cycles.

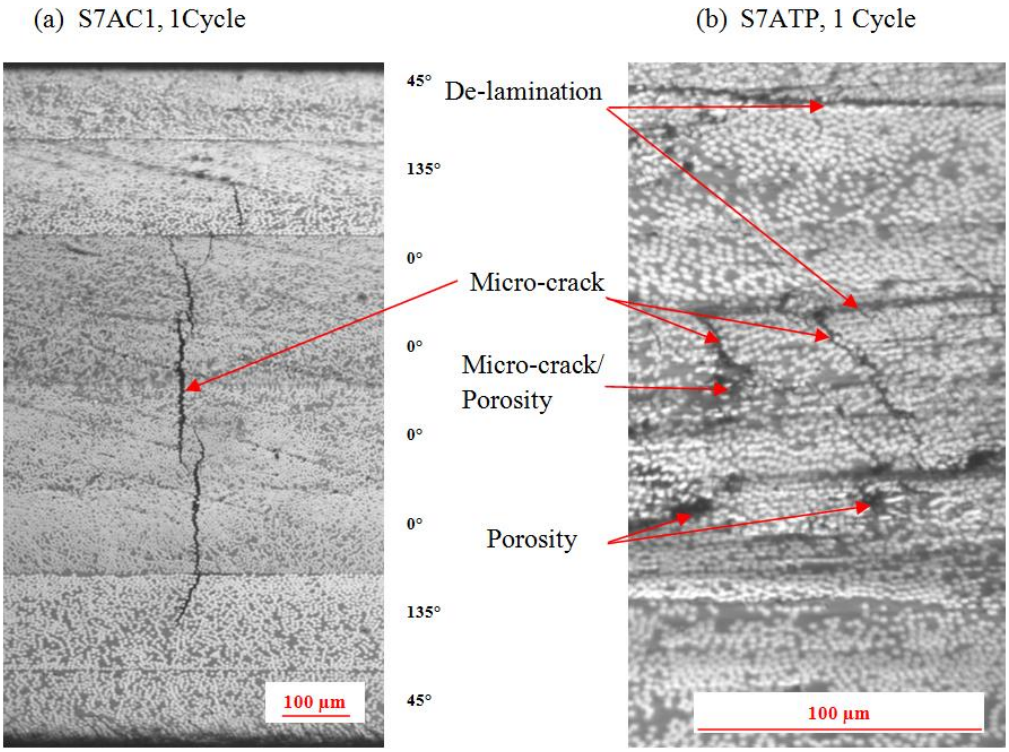

Fig. 18 (a) Micrograph of laminate S7AC1 following one cryogenic cycle, showing a large micro-crack, which propagates through the all four 0° plies and into the 135° plies. (b) Micrograph of laminate S7ATP following one cryogenic cycle which shows de-laminations, micro-cracking, and porosity.

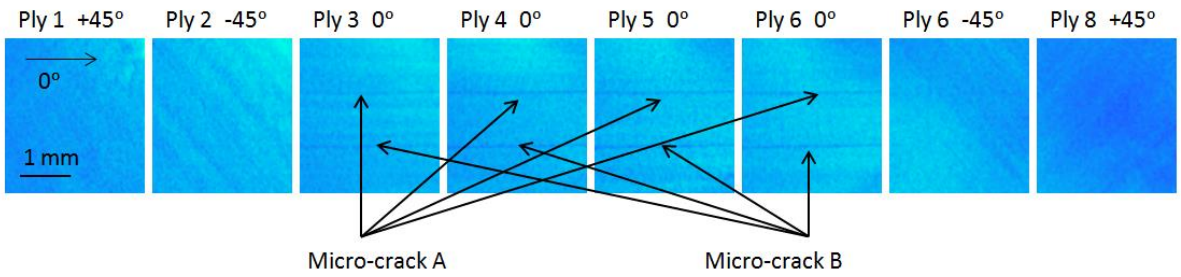

Fig. 19 CT scan of laminate S7AC1 showing ply-by-ply sections of the laminate and micro-cracks A and B in the central plies.

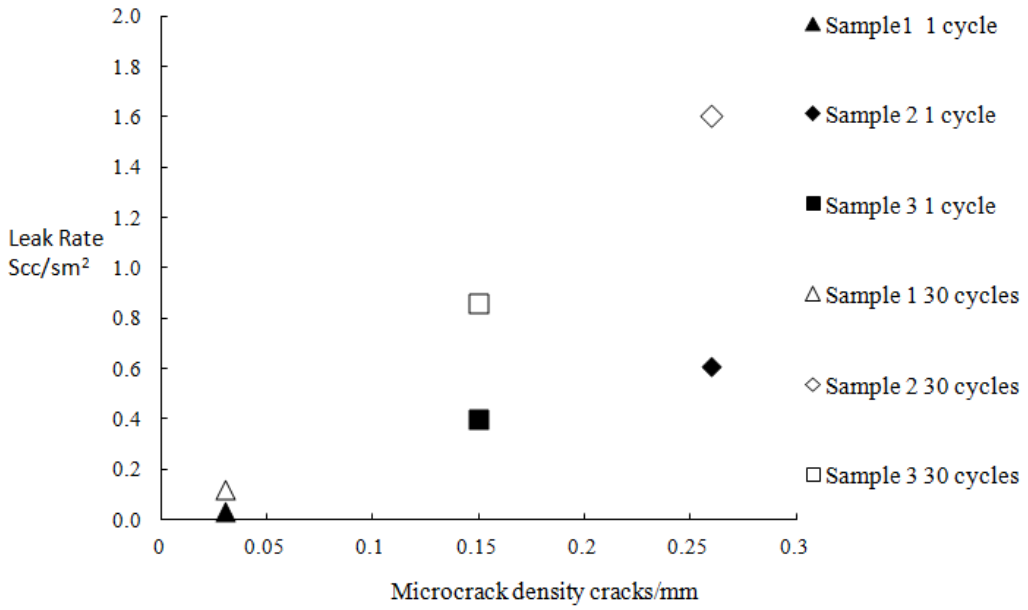

Fig. 20 Leak rate of laminate S7AC1 samples S1, S2 and S3 after cryogenic cycling showing the correlation between measured micro-crack density and leak rate.